The Astronomical Journal, 132:1234–1247, 2006 September

THE SOLAR NEIGHBORHOOD. XVI. PARALLAXES FROM CTIOPI: FINAL RESULTS FROM THE 1.5 m TELESCOPE PROGRAM

Edgardo Costa[1] and René A. Méndez[1]
Departamento de Astronomía, Universidad de Chile, Casilla 36-D, Santiago, Chile; costa@das.uchile.cl, rmendez@das.uchile.cl

W.-C. Jao,[1] Todd J. Henry,[1] and John P. Subasavage[1]
Department of Physics and Astronomy, Georgia State University, Atlanta, GA 30302-4106;
jao@chara.gsu.edu, thenry@chara.gsu.edu, subasavage@chara.gsu.edu

and

Philip A. Ianna[1]
Department of Physics and Astronomy, University of Virginia, Charlottesville, VA 22903; p.ianna@juno.com
Received 2006 April 11; accepted 2006 May 5

ABSTRACT

Trigonometric parallaxes, proper motions and $V_J(RI)_{\rm KC}$ photometry are given for 25 stars (of which one is a zero-parallax control field) targeted by the Cerro Tololo Inter-American Observatory Parallax Investigation (CTIOPI), a widely scoped program aimed at discovering and characterizing nearby stars. The trigonometric parallaxes and proper motions presented are the last that were obtained with the CTIO 1.5 m telescope, which targeted the fainter subset of the CTIOPI input list. First trigonometric parallaxes are given for 22 systems, of which one is within 10 pc (DENIS 0255−4700), and 10 of which are between 10 and 25 pc. At a distance of 4.97 ± 0.10 pc, and with a spectral type of L7.5 V, DENIS 0255−4700 is now the closest known L dwarf. In addition, with $M_V = 24.44$, it is the faintest dwarf with a measured absolute visual magnitude. We present preliminary trigonometric parallaxes for five additional systems worthy of follow-up, and $VRIJHK_S$ photometry and photometric distance estimates for four of them. We also give photometry and distance estimates for 21 other promising targets in our input list for which definitive trigonometric parallaxes were not possible; 13 are likely to be closer than 25 pc. We also present color-magnitude and color-color diagrams, which, in combination with theoretical isochrones from the literature, tangential velocities, and M_R and M_J, have aided to identify the general nature of each of our targets. We have in this way discovered one new (spectroscopically confirmed) subdwarf and two suspected extreme subdwarfs that could be among the most extreme cases of these objects. We have also identified several very low mass stars, a few of which could be brown dwarfs. This concludes the CTIOPI 1.5 m program, from which we have derived a total of 69 trigonometric parallaxes (55 definitive, 6 preliminary, and 8 calibration).

Key words: astrometry — solar neighborhood — stars: distances — stars: fundamental parameters — techniques: photometric

1. INTRODUCTION

The nearest stars, being the brightest examples of their types, provide astronomers with much of our understanding of stellar astronomy. For most types of stars, the fundamental framework of stellar astronomy is built on direct measurements of luminosities, colors, temperatures, and masses of stars in the solar neighborhood. By investigating the luminosity function, mass function, kinematics, and multiplicity of stars in the solar vicinity, we can probe the stellar populations of the Galaxy, determine their contributions to its total mass, and estimate the age of the Galactic disk. Furthermore, a more complete census of the solar neighborhood (including precise distance determinations) is highly desirable for upcoming space-based planetary searches that will require well-constrained target lists.

Potential applications of the nearest stars are, however, hampered by the fact that the faint members of the solar neighborhood are significantly underrepresented. Data from the Research Consortium on Nearby Stars (RECONS)[2] list of stars closer than 10 pc indicates that, assuming that the density of stellar systems within 5 pc carries out to 10 pc, ~35% of the systems within this distance limit remain undiscovered. The problem is obviously worse out to 25 pc, a distance at which the incompleteness is anticipated to be ~60% for the entire sky and nearly 70% for the southern sky (see, e.g., Henry et al. 2002).

Only large trigonometric parallax programs can help remedy this problem, so RECONS started the Cerro Tololo Inter-American Observatory Parallax Investigation (CTIOPI) in 1999, a trigonometric parallax program aimed at discovering some 150 new southern star systems within 25 pc, thereby increasing the population of stars known within that distance by ~20%. This survey is being carried out at the Cerro Tololo Inter-American Observatory (CTIO), Chile, initially under support of the NOAO Surveys Program, supplemented with Chilean time, and currently under SMARTS (Small and Moderate Aperture Research Telescope System).[3]

2. SAMPLE

To make our survey efficient at discovering truly close stars our input target list was refined as much as possible, selecting

[1] Visiting Astronomer, Cerro Tololo Inter-American Observatory. CTIO is operated by the Association of Universities for Research in Astronomy, Inc., under contract to the National Science Foundation.

[2] See http://www.chara.gsu.edu/RECONS/.

[3] See http://www.astro.yale.edu/smarts/.

candidate nearby stars on the basis of "closeness" indicators such as large proper motions (see, e.g., Wroblewski & Costa 2001; Scholz et al. 2002) and/or a photometric or spectroscopic estimate of their distances (see, e.g., Costa & Méndez 2003; Henry et al. 2002; Lodieu et al. 2005).

Our targets were then discriminated essentially on the basis of their apparent brightness, and two working lists were produced: a bright sample ($V \sim 10-15$), observed with the CTIO 0.9 m telescope, and a fainter ($V \sim 15-20$) sample that was observed with the CTIO 1.5 m telescope. The first results from the latter effort (hereafter the 1.5 m CTIOPI) were published in Costa et al. (2005, hereafter C05). Here we present the last trigonometric parallaxes and proper motions resulting from observations carried out during the 1.5 m CTIOPI. For some promising 1.5 m CTIOPI targets for which it was not possible to secure appropriate trigonometric parallax data we present $VRIJHK_S$-based photometric parallaxes.

Table 1 gives the J2000.0 coordinates of *all* the above-mentioned targets together with information to aid in their identification, such as another common name, and spectral types. The coordinates were extracted from Two Micron All Sky Survey (2MASS) scans obtained at an epoch similar to that of our parallax observations. The coordinates have been transformed to epoch 2000.0 using the proper motions obtained in the present investigation (see Table 2) or those from SIMBAD or the literature (when available). The spectral types presented in Table 1 are unpublished classifications obtained by G. Lo Curto et al. (2006, in preparation, hereafter L06), as a result of spectroscopic follow-up observations being carried out with the ESO 3.5 m New Technology Telescope (see below).

Follow-up photometric and spectroscopic observations, necessary to determine accurate optical luminosities and fully characterize the nearby stars discovered, were started more or less simultaneously, using facilities at CTIO, La Silla (ESO), and Las Campanas Observatory (LCO). Here we also present the pertinent photometric data, but the spectroscopy will be published elsewhere (L06) once those observations are completed.

Finding charts for our targets are given on the RECONS Web site. They were made from images taken in the present survey, thereby showing the position of the program stars at a fairly recent epoch. The finders are 8$'$.2 on a side; north is at the top, and east is to the left. They have not been trimmed or centered on the program objects, and therefore show exactly how the parallax frames were taken and how the reference system was defined (see § 3). The red circles indicate the parallax investigation targets, and the green circles indicate the reference stars used in the final reduction.

3. THE ASTROMETRY

Full details of the astrometric procedure can be found in C05 and references therein. In the following subsections we therefore present only a brief description of the observational and reduction procedure.

3.1. *Observations*

The astrometric observations were *all* carried out with the same Tektronix 2048 × 2048 detector (24 μm pixels) attached to the Cassegrain focus of the CTIO 1.5 m telescope in its f/13.5 configuration. This combination gives a scale of 0$''$.2408 pixel^{-1} (see Jao et al. 2003) and a field of $\sim$8$'$.19 × 8$'$.19. Gain and read noise were 2.2 e^- ADU^{-1} and 3.8 e^-, respectively. Analog-to-digital converter saturation occurred at 65,535 ADUs, prior to entering the CCD nonlinear region and before the full well was reached. Only one amplifier was used for readout. All CCD frames were first calibrated using standard IRAF (ver. 2.11.3, NOAO, University of Arizona)[4] tasks. For this purpose, zero exposures and dome flats were taken every night.

In general, the parallax targets were placed more or less near the center of the detector, always aiming to achieve a spatially balanced distribution of reference stars of similar brightness around the target. For this purpose the field around each parallax target was explored in the V, R, and I bandpasses to determine in which filter the brightness of the field stars was comparable to the brightness of the target. Once the best bandpass and positioning for a given field was decided, all subsequent observations were made with the same filter, and the target was placed within a few pixels of the chosen position.

To minimize the effects of differential color refraction (DCR) a great deal of effort was made to take all parallax frames as close as possible to the meridian. Exposure times were kept between a minimum of 30 s (to average out transient atmospheric effects) and a maximum of 1200 s.

Based on previous experience and given the fine scale of the CTIO 1.5 m setup, we anticipated that approximately 30 good frames taken over 2 yr would be adequate to decouple parallax and proper motion, and yield final parallaxes with a precision between 3 and 5 mas. As shown by the results presented in C05 and those presented here, this was indeed confirmed. Furthermore, under certain conditions it was possible to reach our goal within a shorter time period and with fewer frames, with only a moderate increase in the parallax error. The mean error of the final parallaxes presented here (see Table 2) turned out to be 3.42 mas. This higher mean error (compared to the 2.48 mas mean error attained in C05) is consistent with the fainter average brightness of the targets presented in this work (see Table 4) and, in some cases, by a weaker time coverage and/or number of frames.

To check for consistency and detect possible systematic effects, eight parallax calibration stars were observed throughout our program. Results for seven of them were reported in C05, in which we showed that, within the limited number of comparison stars, our results agree well with other parallax determinations. Here we present the observations of the distant ($d \sim 400$ pc) calibration cluster IC 4756 (Herzog et al. 1975), which was targeted to check for possible systematic errors producing spurious parallaxes. As shown by the result given in Table 2 (IC 4756-H165), the parallax for this target is indeed consistent with zero parallax within the observational errors.

3.2. *Reductions*

After sorting all our observations by target, we determined the (X, Y) centroids, the peak flux above background, the ellipticity, and the FWHM of the targets and reference stars in all images using SExtractor (Bertin & Arnouts 1996). The resulting output by SExtractor was then used by a customized program that calculates the parallax factors and takes into account DCR effects to select the frames to be kept for the first iteration in the parallax calculation.

To calculate the parallax factors, precise Earth–to–solar system barycenter distances were obtained from the Jet Propulsion Laboratory (DE405) ephemeris. Recent epoch coordinates were obtained from 2MASS. An empirical model derived by Jao et al.

[4] IRAF is distributed by the National Optical Astronomy Observatory, which is operated by the Association of Universities for Research in Astronomy, Inc., under cooperative agreement with the National Science Foundation.

TABLE 1

Identification of the Targets

ID	Name	R.A. (J2000.0)	Decl. (J2000.0)	Other Common Name	Spectral Type	Notes
1	GJ 2014	00 49 58.63	−26 24 05.6	BPM 46662		
2	APMPM J0207−3722	02 07 14.05	−37 21 50.2	LEHPM 2198	M6.5 V	
3	DENIS 0255−4700	02 55 03.68	−47 00 51.6		L7.5 V	
4	LHS 176	03 35 38.61	−08 29 22.8	LP 653-13		
5	LHS 189	04 25 38.36	−06 52 37.0	LP 655-14		a
6	LHS 190	04 25 38.35	−06 52 37.0	LP 655-15		a
7	LHS 1749 AB	05 16 00.39	−72 14 12.6		M2 V	
8	LHS 1749-Ref4	05 15 45.14	−72 11 22.2			b
9	LHS 1843	06 23 08.84	−32 32 11.6	LP 894-35		
10	WT 207	07 02 36.60	−40 06 28.2		M4.0 V	
11	LHS 2021	08 30 32.57	+09 47 15.5	LP 485-17	M6.5 V	
12	LHS 254	08 54 12.34	−08 05 00.2	LP 666-11		
13	LP 844-33	08 56 17.63	−23 26 57.3	CE 58		
14	LHS 269	09 29 11.08	+25 58 09.4	LP 370-26		
15	2MASS 0952−1924	09 52 21.88	−19 24 32.2		M7.0 V	
16	LHS 2243	10 16 34.69	+27 51 49.0	LP 315-53	M6.5 V	
17	LHS 284	10 36 03.09	−14 42 29.1	LP 730-45		
18	DENIS 1058−1548	10 58 47.84	−15 48 17.2		L4.0 V?	c
19	LHS 2400	11 22 42.54	−32 05 40.4	LP 906-20	M5.0 V	
20	LP 907-010	11 38 50.64	−28 42 30.5	NLTT 28096		
21	DENIS 1151−1202	11 51 09.25	−12 02 00.4			d
22	LHS 323	12 17 30.16	−29 02 20.6	LP 908-41		
23	LHS 326	12 24 26.81	−04 43 36.7	LP 675-8		
24	DENIS 1228−1547	12 28 15.23	−15 47 34.2			d
25	LHS 339	12 40 24.19	−23 17 43.8	LP 853-15	WD	
26	LP 796-012	12 51 55.21	−16 14 11.7	NLTT 32131	M5.0 V	
27	LHS 360	13 46 55.53	+05 42 56.3	LP 558-40	M0.0 VI	
28	LP 912-20	13 51 44.99	−28 21 05.6	NLTT 35463		
29	LHS 2826	13 56 20.56	−28 03 49.8			
30	DENIS 1441−0945	14 41 37.16	−09 45 59.0			
31	DENIS 1456−2747	14 56 01.36	−27 47 37.4			d
32	2MASS 1507−1627	15 07 47.67	−16 27 40.1		L5.0 V	
33	DENIS 1510−0241	15 10 16.86	−02 41 07.9			d
34	LHS 3141 AB	15 59 38.65	−22 25 42.4	LP 861-6		
35	DENIS 1626−0639	16 26 01.35	−06 39 25.8			d
36	LTT 6962	17 33 19.78	−64 20 10.5		M4.0 V	
37	LHS 3370	18 13 52.88	−77 08 20.7	L 44-60	M3.0 V	
38	IC 4756-H165	18 38 18.85	+05 31 02.9			e
39	IC 4756-Ref6	18 38 13.87	+05 29 53.6			f
40	CE 507	18 43 12.38	−33 22 31.3		M6 V	
41	LHS 3451 A	19 19 29.32	−18 19 05.5	LP 812-95		
42	LHS 3451 B	19 19 30.88	−18 19 22.1	LP 812-96		
43	DENIS 2000−7523	20 00 48.42	−75 23 07.0			d
44	MFL2000 J210104.18+030705.1	21 01 04.79	+03 07 04.7			
45	LHS 504	21 05 14.03	−24 46 51.9	LP 872-39	M5.0 V	
46	LHS 505	21 11 57.87	−31 03 15.9	LP 929-8		
47	HB88 M11	21 35 45.54	−42 18 34.4			d
48	2MASS 2206−2047	22 06 22.80	−20 47 05.9		M7.5 V	
49	2MASS 2306−0502	23 06 29.36	−05 02 29.2		M8.0 V	
50	APMPM J2330−4737	23 30 16.16	−47 36 45.1		M7 V	
51	APMPM J2331−2750	23 31 21.75	−27 49 49.6		M7.5 V	
52	APMPM J2344−2906	23 43 32.02	−29 06 27.5		M7 V	
53	APMPM J2359−6246	23 58 42.86	−62 45 42.4	LEHPM 6572		

Note.—Units of right ascension are hours, minutes, and seconds, and units of declination are degrees, arcminutes, and arcseconds.

[a] Double system. Blended in 2MASS, from which the coordinates were extracted.

[b] Nearby star in the field of LHS 1749 AB. Originally our reference star 4.

[c] There is some evidence indicating that this star could be a SD.

[d] No proper motion available to calculate the coordinates at epoch 2000.0.

[e] Confirmed member of the open cluster IC 4756 (Herzog et al. 1975). Star 165 in that work.

[f] Nearby star in the field of IC 4756. Originally our reference star 6.

TABLE 2
Parallax Investigation Results

Name (1)	π_{rel} (mas) (2)	π_{corr} (mas) (3)	π_{abs} (mas) (4)	μ (arcsec yr^{-1}) (5)	P.A. (deg) (6)	N_{fr} (7)	T (yr) (8)	N_{run} (9)	N_{ref} (10)	Filter (11)
Program Stars										
DENIS 0255−4700	201.14 ± 3.89	0.23 ± 0.05	201.37 ± 3.89	1.1485 ± 0.0022	119.5 ± 0.21	44	3.2	9	17	*I*
LHS 1749 AB	44.19 ± 5.08	1.17 ± 0.17	45.36 ± 5.08	0.8355 ± 0.0039	358.3 ± 0.41	34	2.0	7	17	*V*
LHS 1749-Ref4	18.84 ± 5.27	1.17 ± 0.17	20.01 ± 5.27	0.0203 ± 0.0035	203.4 ± 17.9	36	2.0	7	17	*V*
WT 207	38.68 ± 1.32	1.76 ± 0.17	40.44 ± 1.33	0.6320 ± 0.0023	103.2 ± 0.36	56	1.2	7	18	*I*
LHS 2021	59.29 ± 4.52	0.52 ± 0.04	59.81 ± 4.52	0.6720 ± 0.0022	228.1 ± 0.38	19	3.1	6	18	*I*
LP 844-33	40.71 ± 2.94	1.71 ± 0.16	42.42 ± 2.94	0.4154 ± 0.0032	279.6 ± 0.73	29	2.2	5	21	*I*
2MASS 0952−1924	32.93 ± 2.95	0.92 ± 0.07	33.85 ± 2.95	0.1186 ± 0.0021	211.0 ± 1.94	23	2.9	7	20	*I*
LHS 2400	43.67 ± 2.28	0.59 ± 0.05	44.26 ± 2.28	0.6141 ± 0.0021	175.6 ± 0.32	26	1.9	5	18	*R*
LP 796-012	15.22 ± 5.51	0.73 ± 0.09	15.95 ± 5.51	0.4380 ± 0.0049	239.7 ± 1.25	24	2.2	7	17	*I*
LHS 360	9.74 ± 2.85	0.59 ± 0.10	10.33 ± 2.85	1.1428 ± 0.0043	221.1 ± 0.44	23	1.4	4	14	*R*
2MASS 1507−1627	143.62 ± 2.05	0.46 ± 0.08	144.08 ± 2.05	0.9021 ± 0.0017	189.4 ± 0.18	21	2.3	6	19	*I*
LHS 3141 AB	29.50 ± 4.78	1.20 ± 0.14	30.70 ± 4.78	0.5562 ± 0.0061	159.1 ± 1.18	28	1.2	4	19	*R*
LTT 6962	24.38 ± 2.65	1.37 ± 0.17	25.75 ± 2.66	0.6121 ± 0.0024	189.3 ± 0.31	39	2.4	7	22	*I*
IC 4756-Ref6	15.91 ± 2.77	3.58 ± 0.61	19.49 ± 2.84	0.0086 ± 0.0026	175.0 ± ...	41	2.3	5	19	*R*
CE 507	63.45 ± 2.50	2.06 ± 0.21	65.51 ± 2.51	0.3936 ± 0.0024	203.3 ± 0.66	40	2.3	7	20	*I*
LHS 3451 A	21.05 ± 4.06	1.23 ± 0.10	22.28 ± 4.06	0.5074 ± 0.0037	156.8 ± 0.67	29	1.2	4	20	*I*
LHS 3451 B	23.02 ± 4.06	1.23 ± 0.10	24.25 ± 4.06	0.5238 ± 0.0037	156.1 ± 0.65	29	1.2	4	20	*I*
LHS 505	34.51 ± 4.65	1.38 ± 0.20	35.89 ± 4.65	1.0460 ± 0.0046	125.7 ± 0.50	38	2.3	5	19	*I*
2MASS 2206−2047	36.46 ± 3.36	1.03 ± 0.14	37.49 ± 3.36	0.0359 ± 0.0039	148.4 ± 12.0	53	2.6	7	17	*I*
2MASS 2306−0502	81.90 ± 2.58	0.68 ± 0.13	82.58 ± 2.58	1.0358 ± 0.0018	117.1 ± 0.19	45	3.3	8	18	*I*
APMPM J2330−4737	72.06 ± 3.32	0.65 ± 0.19	72.71 ± 3.33	1.1261 ± 0.0026	210.1 ± 0.26	41	3.3	10	18	*I*
APMPM J2331−2750	68.18 ± 2.06	0.96 ± 0.11	69.14 ± 2.06	0.7637 ± 0.0013	5.8 ± 0.15	33	3.3	7	16	*I*
APMPM J2344−2906	30.40 ± 4.54	1.92 ± 0.35	32.32 ± 4.55	0.4077 ± 0.0029	123.2 ± 0.78	31	3.3	6	14	*I*
APMPM J2359−6246	46.94 ± 2.22	1.04 ± 0.14	47.98 ± 2.22	0.5789 ± 0.0025	81.7 ± 0.38	40	2.3	6	22	*I*
Calibration Star										
IC 4756-H165	0.50 ± 2.65	3.56 ± 0.65	4.06 ± 2.73	0.0115 ± 0.0026	198.6 ± 23.1	44	2.3	5	16	*R*

(2005), which requires *VRI* photometry of the targets and parallax reference stars, was used to address DCR corrections. A special version of this model was used in a few cases for which *V*-band photometry could not be obtained for target stars (on account of their extreme faintness in this bandpass).

The least-squares astrometric solution of the multi-epoch frames taken for each target star leads to the determination of its parallax and proper motion. This was achieved using a modified version of the University of Texas program GaussFit (Jefferys et al. 1987). The procedure requires the selection of one of the frames as the trail plate, which defines a fundamental reference system with respect to which all other frames are registered. The true orientation of the trail plate with respect to the International Celestial Reference Frame (ICRF; Arias et al. 1995) was determined by comparison with the Guide Star Catalog, version 2.2.

The photometric parallax method, which requires *VRI* photometry (see § 4) for the reference stars, was used to convert the relative parallax to absolute parallax via relationships between absolute magnitude and color to estimate the distance of the reference stars in each target field. The specific relationships between absolute magnitude and color we used were those established between M_V and the colors $(V-R)$, $(V-I)$, and $(R-I)$ by Henry et al. (2004, hereafter H04), which implicitly assume that all reference stars are dwarfs.

3.3. *Results*

Our astrometry results, together with other relevant data, are given in Tables 2 and 3. In Table 2 we present parallax results that can be considered final, based on the quality of the data available. In Table 3 ("special cases") we present preliminary parallaxes of problematic objects and objects with lower quality observations, which deserve further attention. Both tables have the same format; column (1) gives the names of the targets; column (2), the derived relative parallax and its error; column (3), the correction from relative to absolute parallax and its error; column (4), the absolute parallax and its error; column (5), the proper motion and its error; and column (6), the proper-motion position angle (P.A.) and its error. Columns (7)–(9) give the numbers of parallax frames that were secured for each target, the time spans during which the targets were observed, and the numbers of independent observing runs in which they were visited, respectively. Finally, column (10) gives the number of reference stars used in the final reduction process, and column (11) the filter used for parallax observations, V_J, R_{KC}, or I_{KC}.

A look at Table 2 readily shows that, of the 23 systems with first trigonometric parallaxes reported here, one (DENIS 0255−4700) is within 10 pc, the horizon of the Research Consortium on Nearby Stars, and 10 are between 10 and 25 pc, the classical distance limit of the Catalog of Nearby Stars and the Nearby Stars (NStars) Project.

At a distance of 4.97 ± 0.10 pc, and with a spectral type of L7.5 V (L06; see Table 1), DENIS 0255−4700 is now the closest known L dwarf. The nearest L dwarf known previously was 2MASS 1507−1627 at a distance of 7.33 pc (Dahn et al. 2002, hereafter D02; also reported here). In addition, with $M_V = 24.44$, it is the faintest dwarf with a measured absolute visual magnitude.

TABLE 3
PARALLAX INVESTIGATION RESULTS—SPECIAL CASES

Name (1)	π_{rel} (mas) (2)	π_{corr} (mas) (3)	π_{abs} (mas) (4)	μ (arcsec yr^{-1}) (5)	P.A. (deg) (6)	N_{fr} (7)	T (yr) (8)	N_{run} (9)	N_{ref} (10)	Filter (11)
APMPM J0207−3722	41.44 ± 10.9	0.35 ± 0.04	41.79 ± 10.9	0.4218 ± 0.0046	72.4 ± 1.11	18	3.3	5	15	*I*
LHS 189[a]	45.20 ± 4.29	0.86 ± 0.10	46.06 ± 4.29	1.2040 ± 0.0051	145.7 ± 0.48	35	2.0	6	19	*R*
LHS 190[a]	61.56 ± 4.29	0.86 ± 0.10	62.42 ± 4.29	1.2024 ± 0.0051	146.1 ± 0.48	35	2.0	6	19	*R*
DENIS 1441−0945	35.16 ± 3.49	1.23 ± 0.73	36.39 ± 3.57	0.1987 ± 0.0029	265.5 ± 1.27	17	2.9	5	18	*I*
LHS 3370...............................	41.62 ± 4.25	1.23 ± 0.13	42.85 ± 4.25	0.7510 ± 0.0063	198.8 ± 0.81	18	1.3	4	23	*R*
LHS 504.................................	11.74 ± 4.43	0.63 ± 0.07	12.37 ± 4.43	1.1009 ± 0.0020	197.6 ± 0.15	32	2.8	5	19	*I*

[a] Double system. Partially resolved at the scale of the astrometry observations. See § 3.4 for full discussion.

DENIS 0255−4700 is a promising object for upcoming extrasolar planetary searches from space.

To the best of our knowledge, only one of the objects presented in Table 2, 2MASS 1507−1627, has been the subject of an independent trigonometric parallax investigation. D02 obtained an absolute parallax value of 136.4 ± 0.6 mas for this star, a value which is in fair agreement with ours (144.08 ± 2.05 mas). Their proper-motion and position-angle data (0.″9031 ± 0.″0005 yr^{-1} and 190.°3 ± 0.°1, respectively) agree well with ours (0.″9021 ± 0.″0017 yr^{-1}, 189.°4 ± 0.°18). It should be noted that their results are based on a significantly larger number of observations.

3.4. *Notes on Individual Objects*

"Inhomogeneous reference frame" refers to a situation in which many of the reference stars are located on one side of the target star field (finders can be found in the RECONS Web site). We consider this situation potentially detrimental to the quality of the astrometry. Details for stars worthy of notice are given here in order of right ascension.

APMPM J0207−3722.—Preliminary parallax is reported because this system has an unexplained huge error (10.9 mas) in the parallax. It has a good time base and sampling of the parallax orbit in spite of the moderate number of frames available. It could lie within the NStars horizon ($d \sim 25$ pc).

LHS 189/190.—This multiple system consists of two known components of similar brightness ($\Delta R \sim 0.5$ mag) separated by ∼3″. At the scale of our setup (0.″24 $pixel^{-1}$) this combination of brightness and separation caused an unsolvable reduction challenge, which is reflected by the fact that we have obtained different parallax values for each component—a highly unlikely possibility. Of the two results given in Table 3, probably that of the brighter component (LHS 189) is closer to the true value for the system. We have included this object in Table 3 to draw attention to the fact that this system is relatively nearby and deserves observation with a higher resolution.

LHS 1749 AB.—This star was discovered to be a nearby multiple by the CTIO 0.9 m CTIOPI program (Jao et al. 2003). It is currently being observed by the CTIOPI under the SMARTS program to determine if the atypically large error (±5.08 mas; this in spite of the high-quality data available) of the 1.5 m CTIOPI result and some trends seen in the 1.5 m residual plots are being caused by the known faint ($\Delta V \sim 3$ mag) secondary component at ∼2.″9, or by an unknown third companion. Although the reference frame is fairly inhomogeneous, we believe this is not the cause of the effect seen.

LHS 1749-Ref4.—This star, originally our parallax investigation reference star 4 in the frames of LHS 1749 AB, was discovered by chance to be nearby ($d \sim 50$ pc). This star is located in one corner of our frames; therefore, the parallax reference frame used must be considered very inhomogeneous and could be affecting our distance determination. See discussion below for IC 4756-H165 and IC 4756-Ref6.

LP 796-012.—This has an unexplained, atypically large error of 5.51 mas in the parallax. Sampling of the parallax orbit was good in spite of the moderate number of frames available.

DENIS 1441−0945.—Preliminary parallax is reported because of the small number of frames available for this system. In absence of appropriate *V*-band photometry of the parallax reference stars in this field, a single relation of M_R versus $R - I$ was used to determine the reference star distances. Single stars in the RECONS sample with parallaxes having errors less than 5 mas were used to generate the relation, after removing white dwarfs (WDs), subdwarfs (SDs), and evolved stars (i.e., subgiants). It seems to be nearby ($d \sim 27$ pc).

LHS 3370.—Preliminary parallax reported because of the small number of frames available and the short time base of our observations. It seems to lie within the NStars horizon ($d \sim 25$ pc).

IC 4756.—This is an open cluster at a distance of ∼400 pc that has been studied by Herzog et al. (1975). Only two stars with photometry and proper motions in that paper coincide with stars selected as parallax reference stars in our study. Of the two, Herzog 165 (IC 4756-H165) was chosen as the parallax target because it had the highest probability of cluster membership. This star is located in one corner of our frames; therefore, the parallax reference frame used must be considered as very inhomogeneous. We do not see, however, any evidence of systematic effects in our result because of this situation. The second highest probability cluster member (Herzog 181), which is better located with respect to the reference stars, was also tested as a parallax target, giving an almost identical result.

IC 4756-Ref6.—This star, originally our parallax investigation reference star 6 in the frames of IC 4756, was discovered by chance to be nearby ($d \sim 51$ pc). Although less extreme a case than that of IC 4756-H165, the reference frame used must also be considered as very inhomogeneous and could be affecting our distance determination. Based on the evidence presented for IC 4756-H165, we believe, however, that this is not the case. Please note the extreme value of the correction from relative to absolute parallax (3.58 ± 0.61), indicating that quite a few of our parallax reference stars may not be very distant, or that they are not main-sequence dwarfs (see § 3.2).

LHS 504.—Preliminary parallax is reported because, in spite of the fairly large number of frames available and the good time base of our observations, the sampling of the parallax ellipse was poor.

APMPM J2331−4737.—Inhomogeneous reference frame.

APMPM J2331−2750.—Inhomogeneous reference frame.

APMPM J2359−6246.—Inhomogeneous reference frame.

4. THE PHOTOMETRY

4.1. *Observations and Reductions*

Full details of the photometric procedure can be found in C05.

As explained in the astrometry section, our pipeline requires knowledge of the *VRI* colors of the targets and the parallax reference stars to address DCR and the correction from relative to absolute parallax.

The photometry was carried out with the Danish 1.54 m telescope at La Silla (ESO), the 1.5 and 0.9 m telescopes at CTIO, and the 1.0 m telescope at LCO. An EEV/MAT 2048 $\times$ 4096 CCD with Bessell *VR* and Gunn *i* filters was used at ESO, a Tektronix 2048 $\times$ 2046 CCD with Tek filters was used at both the CTIO 0.9 and 1.5 m, and a SITe 2048 $\times$ 3150 CCD with Harris filters was used at LCO. Care was taken to choose from whatever sets of filters were available at each site those known to reproduce the standard *VRI* Johnson-Kron-Cousins system best.

The CCD frames were first calibrated using standard IRAF tasks. For this purpose, zero-exposure frames and twilight sky flats were taken every night. Aperture photometry was then performed on each object of interest using the IRAF APPHOT package. The optimum aperture size for each night was determined by means of the IRAF *mkapfile* task. The best aperture radius turned out to be 4–5 times the average FWHM of the frames. A few targets turned out to have stars close enough to be included in the ideal aperture chosen to do the photometry, thereby contaminating the instrumental magnitudes. These cases were treated as explained in C05.

Typically six *UBVRI* standard star areas from the catalogs of Landolt (1992) and Graham (1982) were observed multiple times each night to determine the transformation of our instrumental magnitudes to the standard *VRI* system and to determine atmospheric extinction. To put our observations into the standard system, we used the transformation equations given in C05. The equations were applied to the Landolt/Graham standard star magnitudes, and solved using the IRAF *fitparams* task. Finally, these transformation equations, with their corresponding calculated coefficients, were applied to our program stars by means of the IRAF *invertfit* task, which produces a set of calibrated magnitudes and colors.

4.2. *Results*

The results of our *VRI* photometry for the target stars are presented in Table 4. Column (1) gives the name of the targets; columns (2)–(4) give their average *VRI* magnitudes (we give magnitudes instead of colors mainly for comparison purposes; they were obtained directly from the IRAF output); and columns (5)–(7) give the corresponding standard deviation for all cases with at least three independent measurements. These errors have to be interpreted with caution; it must be kept in mind that they have been derived from a small number of independent observations, and, furthermore, that some of our targets could be variable. In the case of objects with one observation (in one or more filters), the errors were obtained adding in quadrature the IRAF-computed errors for the object, with average values of all other known sources of uncertainty (including the error arising from the fit to the standard stars, and the probable measurement error estimated from our overall photometry). The IRAF-computed errors were not used directly, because, as pointed out by Bucciarelli et al. (2001), the final photometric error computed by *invertfit* does not rigorously treat error propagation, therefore producing a lower limit of the photometric errors. Finally, column (8) gives the number of times the star was observed. We do not present the *VRI* photometry of the parallax reference stars here, but it is available on request.

As can be deduced from Table 4, obtaining reliable *V*- and *R*-band photometry of our reddest, and therefore faintest in *V* and *R*, targets with 1.5 m class telescopes was a challenge. This was possible only in particularly stable atmospheric conditions and with subarcsecond seeing. As a consequence, we were not able to secure *V*-band photometry for a few of them. In the case of DENIS 0255−4700 and 2MASS 1507−1627, being the closest and potentially the most interesting objects of our sample, the photometry was made with the ESO 3.6 m telescope (courtesy of G. Lo Curto). DENIS 0255−4700 was successfully observed with different telescopes in the *I* band, in which it seems to show variability at a level of 0.15 mag.

In Table 5 we give the $IJHK_S$ infrared data available for our targets, extracted from the 2MASS and the Deep Near Infrared Survey of the Southern Sky (DENIS), together with the corresponding 2MASS and DENIS identifications. Part of these imported data were used for comparison purposes and to construct color-magnitude and color-color diagrams (see § 6); the rest are included for completeness. Figure 1 shows the good agreement existing between our Kron-Cousins *I*-band photometry ($I_{\rm our}$) and Gunn *i* DENIS ($I_{\rm DEN}$) observations. For this comparison we have combined the data given here with that published in C05 (it should be noted, furthermore, that at the time of writing C05 only 12 of our targets had published DENIS photometry; the number of objects in common has increased considerably with DENIS's third release). For the 55 objects in common we obtain $\langle I_{\rm DEN} - I_{\rm our}\rangle = 0.021 \pm 0.126$ mag. As can be seen from Figure 1, there is no obvious dependence with *I*, but a small trend with $(R - I)$ is suggested.

5. PHOTOMETRIC DISTANCES

Using our *VRI* photometry and JHK_S photometry from 2MASS, we have determined photometric distance estimates for those 1.5 m CTIOPI targets for which it was not possible to carry out trigonometric parallax observations, as well as for those objects presented in Table 3 (when applicable).

To compute the photometric distances, we used a subset of the multiple relationships between absolute magnitude and color developed by H04, using the RECONS sample of photometrically single main-sequence stars closer than 10 pc, supplemented with a subset of late-type M dwarfs closer than 25 pc (see Table 2 in H04). Specifically, and following the recommendations given in H04, we adopted the 12 M_{K_S} versus color relationships developed for red dwarfs (RDs) with $M_{K_S} \sim 4$–11, corresponding to spectral types K0.0 V to M9.5 V.

In Table 6 we present the corresponding average photometric distances and their standard deviations together with the number ($N_{\rm rel}$; see below) of relationships used for each star. The errors given represent the "internal" error for each star and do not include the error emanating from dispersion of the fits to the M_{K_S} versus color data to establish the numerical relationships used. The comparison between photometric and trigonometric distances for 140 stars presented in H04 indicates that this "external" error amounts to ~15% in the case of RDs, and to ~13% in the case of WDs. In general, there is a good agreement between the distances derived for a given object from different H04 relationships; in all cases the differences are within 3 σ of the estimated distance dispersion.

It should be noted that, based on the applicability range of these relationships (see Table 3 in H04), the availability of *V*-band observations, and other considerations related to the quality of

TABLE 4
OPTICAL PHOTOMETRY

Name (1)	V (2)	R (3)	I (4)	σ_V (5)	σ_R (6)	σ_I (7)	N_{obs} (8)
GJ 2014	14.591	14.282	13.944	0.010	0.008	0.023	5
APMPM J0207−3722	19.388	17.443	14.905	0.045	0.060	0.057	1
DENIS 0255−4700	22.921	19.906	17.454	0.121	0.039	0.031	1[a]
LHS 176	15.885	14.263	12.306	0.010	0.002	0.013	3
LHS 189/190[b]	14.252	13.191	11.977	0.028	0.028	0.028	1
LHS 1749 AB	11.709	10.676	9.430	0.009	0.008	0.014	4
LHS 1749-Ref4	16.496	15.755	15.086	0.040	0.023	0.062	4
LHS 1843	16.240	15.111	13.722	0.008	0.003	0.001	2
WT 207	15.164	13.886	12.275	0.011	0.014	0.026	4
LHS 2021	19.063	17.160	14.774	0.032	0.012	0.003	2
LHS 254	17.156	15.516	13.448	0.022	0.022	0.022	1
LP 844-33	15.978	14.429	12.551	0.007	0.016	0.055	2
LHS 269	16.457	14.808	12.847	0.021	0.022	0.021	1
2MASS 0952−1924	18.349	16.402	14.199	0.001	0.017	0.069	2
LHS 2243	18.946	16.858	14.555	0.004	0.009	0.013	2
LHS 284	16.817	15.507	13.864	0.021	0.022	0.022	1
DENIS 1058−1548	...	20.095	17.764	...	0.019	0.014	2
LHS 2400	16.370	14.816	12.912	0.017	0.010	0.024	3
LP 907-010	18.220	16.471	14.341	0.030	0.026	0.052	2
DENIS 1151−1202	22.569	19.775	17.170	0.038	0.017	0.076	4
LHS 323	16.901	15.700	14.050	0.042	0.024	0.040	2
LHS 326	14.934	13.985	13.052	0.020	0.020	0.020	1
DENIS 1228−1547	...	20.187	18.163	...	0.209	0.065	3
LHS 339	16.529	16.136	15.732	0.018	0.014	0.023	3
LP 796-012	16.992	15.616	13.889	0.012	0.018	0.044	3
LHS 360	15.223	14.290	13.410	0.009	0.010	0.019	3
LP 912-20	17.017	15.773	14.153	0.021	0.022	0.021	1
LHS 2826	15.262	13.869	12.136	0.014	0.040	0.017	4
DENIS 1441−0945	...	20.030	17.234	...	0.021	0.020	2
DENIS 1456−2747	20.969	18.649	16.262	0.087	0.042	0.020	3
2MASS 1507−1627	22.136	18.928	16.579	0.1:	0.097	0.079	5[c]
DENIS 1510−0241	20.505	18.035	15.664	0.080	0.046	0.047	4
LHS 3141 AB	14.267	13.221	11.989	0.011	0.019	0.098	2
DENIS 1626−0639	20.476	17.990	15.393	0.049	0.061	0.047	4
LTT 6962	14.496	13.256	11.753	0.013	0.022	0.018	2
LHS 3370	15.376	14.114	12.545	0.024	0.010	0.024	3
IC 4756-H165	13.591	13.110	12.650	0.008	0.006	0.008	6
IC 4756-Ref6	15.224	14.573	13.977	0.013	0.018	0.012	8
CE 507	16.282	14.621	12.648	0.006	0.015	0.024	4
LHS 3451 A	14.694	13.619	12.279	0.010	0.005	0.074	5
LHS 3451 B	16.384	15.146	13.567	0.025	0.021	0.100	5
DENIS 2000−7523	21.157	18.379	16.119	0.008	0.001	0.024	3
MFL2000 J210104.18+030705.1	18.759	16.547	14.238	0.037	0.038	0.039	1
LHS 504	17.829	16.402	14.856	0.117	0.041	0.050	5
LHS 505	16.262	14.851	13.180	0.034	0.004	0.045	2
HB88 M11	17.180	15.630	13.689	0.035	0.019	0.016	4
2MASS 2206−2047	19.788	17.452	14.877	0.203	0.035	0.163	4
2MASS 2306−0502	18.798	16.466	14.024	0.082	0.065	0.115	5
APMPM J2330−4737	18.081	15.867	13.682	0.020	0.016	0.006	4
APMPM J2331−2750	19.072	16.540	14.190	0.012	0.087	0.016	4
APMPM J2344−2906	19.961	17.811	15.409	0.234	0.028	0.018	2
APMPM J2359−6246	16.954	15.260	13.297	0.028	0.017	0.020	4

[a] Relative photometry made with the ESO 3.6 m telescope.
[b] Double system. Blended at the scale of our optical photometry.
[c] Relative V photometry. Only one V observation made with the ESO 3.6 m telescope.

the photometry, not all of them could be applied to all our objects. Furthermore, there are two cases of stars with bluish colors that are clear outliers: LHS 339, a known WD, and GJ 2014, a suspected SD. In the case of LHS 339, a photometric estimate of its distance was obtained using the empirical relation given in Salim et al. (2004), derived from the Bergeron et al. (2001) photometry for WDs with trigonometric parallaxes.

The reddest objects in our sample also fall within the applicability range of the single relation for dwarfs with spectral types M6.5 through L8 given in D02; for them we present photometric distance estimates from the both the H04 relationships and the D02 relation (in general, only a few of the H04 relationships apply to extremely red stars; see Table 6). With the exception of DENIS 1058−1548 and DENIS 1228−1547, there is good agreement

TABLE 5
INFRARED PHOTOMETRY FROM 2MASS AND DENIS

Name	2MASS							DENIS						
	ID	J	Err_J	H	Err_H	K_S	Err_K	ID	I	Err_I	J	Err_J	K_S	Err_K
GJ 2014	00495863-2624055	13.516	0.029	13.274	0.032	13.136	0.034	J004958.6-262405	13.892	0.060	13.540	0.120	13.083	0.200
APMPM J0207−3722	02071403-3721502	12.439	0.027	11.828	0.026	11.382	0.026	J020713.9-372150	15.066	0.040	12.397	0.080	11.299	0.080
DENIS 0255−4700	02550357-4700509	13.246	0.027	12.204	0.024	11.558	0.024	J025503.3-470049	17.207	0.130	13.212	0.070	11.494	0.090
LHS 176	03353849-0829223	10.377	0.022	9.801	0.022	9.456	0.019	J033538.5-082922	12.725	0.110	10.829	0.120	9.939	0.150
LHS 189/190[a]	04253829-0652357	11.142	0.050	10.658	0.062	10.311	0.037	J042538.3-065236	12.137	0.030	10.948	0.060	10.253	0.080
LHS 1749 AB	05160040-7214135	8.209	0.037	7.623	0.031	7.362	0.024	J051600.3-721415	9.513	0.020	8.170	0.060	...	...
LHS 1749-Ref4	05154514-7211221	14.048	0.029	13.303	0.034	13.211	0.040	J051545.1-721122	15.121	0.050	14.137	0.090	12.824	0.210
LHS 1843	06230879-3232112	12.363	0.023	11.876	0.021	11.659	0.024	J062308.6-323209	13.652	0.020	12.455	0.070	11.724	0.090
WT 207[b]	07023654-4006281	10.736	0.022	10.256	0.025	9.961	0.019	J070236.4-400627	12.203	0.020	10.759	0.060	9.928	0.080
WT 207	...	...	...	...	...	...	...	J070236.4-400628	12.373	0.020	10.705	0.060	9.968	0.070
LHS 2021	08303256+0947153	11.890	0.022	11.165	0.021	10.756	0.023	...	...	...	...	...	...	...
LHS 254	08541227-0804594	11.560	0.024	11.083	0.024	10.810	0.023	...	...	...	...	...	...	...
LP 844-33	08561768-2326574	10.696	0.023	10.126	0.023	9.818	0.021	J085617.6-232657	12.503	0.030	10.704	0.070	9.765	0.070
LHS 269	09291113+2558095	10.906	0.023	10.310	0.023	9.958	0.018	...	...	...	...	...	...	...
2MASS 0952−1924	09522188-1924319	11.865	0.025	11.256	0.024	10.869	0.022	J095221.9-192432	14.165	0.040	11.859	0.080	10.886	0.090
LHS 2243	10163470+2751497	11.987	0.019	11.331	0.022	10.955	0.018	...	...	...	...	...	...	...
LHS 284	10360321-1442300	12.283	0.023	11.793	0.025	11.583	0.028	J103603.2-144230	13.846	0.020	12.195	0.060	11.509	0.100
DENIS 1058−1548[c]	10584787-1548172	14.155	0.035	13.226	0.025	12.532	0.029	...	...	...	...	...	...	...
LHS 2400[b]	11224253-3205398	11.036	0.024	10.519	0.026	10.167	0.019	J112242.4-320538	12.923	0.020	11.138	0.070	10.176	0.080
LHS 2400	...	...	...	...	...	...	...	J112242.5-320537	12.989	0.030	11.070	0.070	10.346	0.070
LP 907-010	11385065-2842306	12.193	0.021	11.620	0.024	11.258	0.019	J113850.6-284230	14.283	0.040	12.272	0.070	11.300	0.080
DENIS 1151−1202	11510924-1202004	14.541	0.042	13.928	0.041	13.396	0.047	J115109.3-120200	17.204	0.130	14.535	0.110	...	...
LHS 323	12173029-2902205	12.544	0.024	12.050	0.024	11.778	0.023	J121730.1-290220	13.965	0.030	12.513	0.060	11.632	0.100
LHS 326	12242688-0443361	11.927	0.022	11.430	0.021	11.234	0.023	J122427.0-044334	12.996	0.030	11.930	0.070	11.149	0.080
DENIS 1228−1547	12281523-1547342	14.378	0.030	13.347	0.032	12.767	0.030	J122815.2-154733	17.886	0.200	14.335	0.100	12.721	0.130
LHS 339	12402426-2317424	15.354	0.047	15.080	0.080	14.936	0.114	J124024.3-231741	15.713	0.050	15.222	0.130	...	...
LP 796-012	12515525-1614113	12.219	0.026	11.683	0.022	11.425	0.024	J125155.3-161410	14.008	0.030	12.215	0.080	11.527	0.100
LHS 360	13465551+0542562	12.390	0.027	11.849	0.026	11.662	0.023	...	...	...	...	...	...	...
LP 912-20	13514501-2821054	12.608	0.028	12.001	0.022	11.744	0.023	J135144.9-282105	14.125	0.030	12.582	0.090	11.699	0.090
LHS 2826	13562062-2803497	10.480	0.026	9.875	0.023	9.565	0.019	...	...	...	...	...	...	...
DENIS 1441−0945	14413716-0945590	14.020	0.029	13.190	0.031	12.661	0.030	J144137.2-094558	17.413	0.130	14.126	0.100	12.530	0.120
DENIS 1456−2747	14560135-2747374	13.250	0.026	12.655	0.024	12.189	0.022	J145601.3-274736	16.423	0.110	13.181	0.090	12.177	0.090
2MASS 1507−1627	15074769-1627386	12.830	0.027	11.895	0.024	11.312	0.026	J150747.6-162740	16.686	0.110	12.869	0.080	11.306	0.070
DENIS 1510−0241	15101685-0241078	12.614	0.023	11.842	0.022	11.347	0.021	J151016.8-024107	15.736	0.060	12.820	0.070	11.339	0.080
LHS 3141 AB	15593863-2225420	10.832	0.023	10.314	0.024	10.124	0.019	J155938.6-222540	12.028	0.020	10.927	0.060	10.065	0.070
DENIS 1626−0639	16260134-0639257	12.837	0.023	12.211	0.023	11.846	0.024	J162601.3-063926	15.541	0.070	12.909	0.090	11.748	0.100
LTT 6962	17331977-6420107	10.365	0.028	9.761	0.030	9.506	0.029	...	...	...	...	...	...	...
LHS 3370[d]	18135285-7708209	11.132	0.023	10.618	0.025	10.352	0.020	J181352.7-770821	12.901	0.040	11.538	0.090	10.640	0.080
LHS 3370[e]	...	...	...	...	...	...	...	J181352.7-770821	12.534	0.030	11.075	0.070	10.322	0.070
IC 4756-H165	18381386+0529535	12.030	0.023	11.711	0.023	11.585	0.023	...	...	...	...	...	...	...
IC 4756-Ref6	18381884+0531028	13.215	0.026	12.783	0.031	12.569	0.032	...	...	...	...	...	...	...
CE 507[f]	18431237-3322313	10.732	0.032	10.140	0.030	9.829	0.024	J184312.3-332231	12.788	0.030	10.835	0.080	9.942	0.070
LHS 3451 A	19192930-1819047	11.020	0.025	10.523	0.025	10.327	0.027	J191929.3-181904	12.295	0.020	11.023	0.060	10.297	0.060
LHS 3451 B	19193085-1819214	12.200	0.025	11.677	0.025	11.456	0.026	J191930.8-181921	13.621	0.030	12.215	0.070	11.360	0.070
DENIS 2000−7523[b]	20004841-7523070	12.734	0.026	11.967	0.027	11.511	0.026	J200048.3-752306	15.900	0.060	12.753	0.070	11.466	0.090
DENIS 2000−7523	...	...	...	...	...	...	...	J200048.3-752306	15.882	0.060	12.654	0.080	11.468	0.090

TABLE 5—*Continued*

Name	2MASS ID	2MASS J	2MASS Err_J	2MASS H	2MASS Err_H	2MASS K_S	2MASS Err_K	DENIS ID	DENIS I	DENIS Err_I	DENIS J	DENIS Err_J	DENIS K_S	DENIS Err_K
MFL2000 J210104.18+030705.1	21010483+0307047	11.704	0.023	10.961	0.024	10.567	0.024	...	...	...	...	...	...	...
LHS 504	21051406-2446504	13.355	0.033	12.889	0.041	12.630	0.038	J210514.0-244651	14.765	0.040	13.373	0.080	12.587	0.120
LHS 505	21115778-3103151	11.622	0.026	11.101	0.025	10.844	0.027	J211157.8-310315	13.167	0.070	11.661	0.080	10.814	0.070
HB88 M11	21354554-4218343	11.682	0.021	11.147	0.025	10.809	0.021	...	...	...	...	...	...	...
2MASS 2206−2047	22062280-2047058	12.370	0.022	11.684	0.022	11.315	0.027	J220622.7-204706	15.087	0.040	12.421	0.070	11.198	0.070
2MASS 2306−0502	23062928-0502285	11.354	0.022	10.718	0.021	10.296	0.023	...	...	...	...	...	...	...
APMPM J2330−4737	23301612-4736459	11.229	0.024	10.641	0.025	10.279	0.021	J233016.2-473642	13.703	0.040	11.321	0.060	10.316	0.070
APMPM J2331−2750[b]	23312174-2749500	11.646	0.023	11.055	0.026	10.651	0.026	J233121.7-274949	14.249	0.040	11.658	0.070	10.619	0.080
APMPM J2331−2750	...	...	...	...	...	...	...	J233121.7-274950	14.258	0.040	11.654	0.110	10.632	0.130
APMPM J2344−2906	23433198-2906271	13.256	0.028	12.754	0.024	12.433	0.030	...	...	...	...	...	...	...
APMPM J2359−6246	23584285-6245423	11.387	0.026	10.827	0.023	10.515	0.023	J235842.8-624542	13.305	0.030	11.406	0.070	10.435	0.070

[a] Double system. Blended in 2MASS and DENIS.
[b] Two entries in DENIS third edition.
[c] Not included in final DENIS releases.
[d] In second edition of DENIS.
[e] In third edition of DENIS.
[f] Not included in third edition of DENIS release; value from second release.

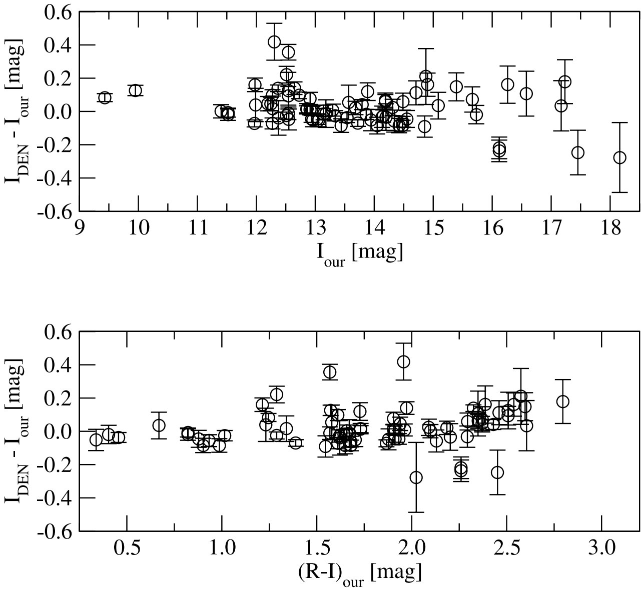

Fig. 1.—Comparison of our Kron-Cousins *RI* photometry with DENIS Gunn *i* photometry. The error bars represent the square root of the DENIS error and our error added in quadrature.

between both results. Direct comparison of the photometric distances presented in Table 6 for these two stars, with the trigonometric distances given for them in D02 (17.3 pc for DENIS 1058−1548 and 20.2 pc for DENIS 1228−1547), shows that in both cases the D02 relation reproduces best the true (trigonometric) distance. In general, this could be explained by the fact that the only relationship from H04 applicable to these two objects [M_{K_S} vs. $(R-I)$] has a narrower color base than the D02 relation [which uses $(I-J)$], and therefore is more sensitive to photometric uncertainties. (We would like to note that the H04 relationships are meant to be used as an ensemble to reduce the effect of photometric errors, something that was not possible for these two stars.) In the case of DENIS 1058−1548 comparison is straightforward, but in the case of DENIS 1228−1547 interpretation of the photometric distances is complicated by the fact that this object is a close binary system with nearly equal brightness components (Martin et al. 1999) and by the high uncertainty of our *R* magnitude (see Table 4). If duplicity is taken into account (the data presented in Table 6 ignore its effect), and it is assumed that the components are identical, the photometric distance obtained using the D02 relation and the photometry given in D02 (whose declared errors are smaller than ours for this particular object) turns out to be 19.6 pc, in very good agreement with the trigonometric distance.

As indicated in Table 1, we have evidence that DENIS 1058−1548 could be a SD (L06). If this were the case, the photometric distances given in Table 6 (derived assuming that it is a main-sequence dwarf) would be overestimations of the true distance. Interestingly, the photometric distances presented are in fact larger than the trigonometric distance given by D02. We expect to obtain an infrared spectrum in the near future to settle this matter.

6. COLOR-MAGNITUDE AND COLOR-COLOR DIAGRAMS

In this section we present selected color-magnitude diagrams (CMDs) and color-color diagrams (CoCoDs), which, in combination with theoretical isochrones from the literature and other derived properties of the observed sample, have aided in identifying the general nature of our targets.

TABLE 6
Mean Photometric Distances

Name	Distance (pc)	σ[a] (pc)	N_{rel}
APMPM J0207−3722	20.7	0.9	11
LHS 176	13.3	0.8	12
LHS 1843	102.3	7.8	12
LHS 254	25.6	4.0	12
LHS 269	16.4	0.9	12
LHS 2243	16.9	0.5	12
LHS 284	64.7	6.9	12
DENIS 1058−1548	33.3	...	1
DENIS 1058−1548[b]	21.0	...	1
LP 907-010	24.7	1.0	12
DENIS 1151−1202	45.7	5.2	8
LHS 323	77.2	6.5	12
LHS 326	138.9	9.4	10
DENIS 1228−1547	54.1	...	1
DENIS 1228−1547[b]	17.1	...	1
LHS 339[c]	24.8	...	1
LP 912-20	69.3	1.2	12
LHS 2826	20.3	1.0	12
DENIS 1441−0945	28.3	0.6	3
DENIS 1441−0945[b]	33.4	...	1
DENIS 1456−2747	26.0	1.1	12
DENIS 1456−2747[b]	27.9	...	1
DENIS 1510−0241	16.4	1.3	10
DENIS 1510−0241[b]	20.2	...	1
DENIS 1626−0639	23.7	1.5	9
LHS 3370	44.0	5.4	12
DENIS 2000−7523	16.8	2.8	6
DENIS 2000−7523[b]	15.2	...	1
MFL2000 J210104.18+030705.1	13.9	0.5	12
LHS 504	117.2	20.2	12
HB88 M11	25.0	0.8	12

[a] Internal error. See text for discussion on external error sources.
[b] From D02, for very late spectral types (≥M6.5).
[c] From Salim et al. (2004), for WDs.

In Figure 2 we present two CMDs: an M_R versus $R-I$ CMD constructed with *RI* data from the present survey and an M_J versus $I-J$ CMD constructed combining our *I*-band data with *J*-band data from 2MASS. Other magnitude-color combinations tested did not show significant differences. The absolute magnitudes M_R and M_J, and their associated errors σ_{M_R} and σ_{M_J}, were computed as indicated in C05. The color error bars represent the square root of the corresponding magnitude errors added in quadrature.

For interpretation purposes, we have superposed various theoretical isochrones on our CMDs. We present two sets of solar metallicity ($Z = 0.019$, $[Fe/H] = 0$) isochrones from models by Chabrier et al. (2000), one for very low mass stars (VLMs) and another for brown dwarfs (BDs). The thin solid line is for 0.1 Gyr objects (VLM+BD in Fig. 2), and the dotted line is for 5.0 Gyr objects (VLM in Fig. 2). Both sets of models were computed for masses below 0.1 $M_\odot$. The transition between VLMs and BDs in these models occurs for a mass of $\sim$0.07 $M_\odot$. For illustration purposes we have included in the figures a few mass values from the models (labels to the right correspond to the 0.1 Gyr isochrones, those to the left to the 5.0 Gyr isochrones). Note that the most massive BDs (0.07 $M_\odot$) have $M_R \sim 13.6$ and $M_J \sim 9.8$ for an age of 0.1 Gyr. The same massive BDs fade to $M_R \sim 22.1$ and $M_J \sim 15.2$ for an age of 5.0 Gyr.

We also present isochrones for 4.5 Gyr solar-metallicity RDs, from models by Baraffe et al. (1998) (Fig. 2, *thick solid lines*). These isochrones also extend to very low masses, but in order

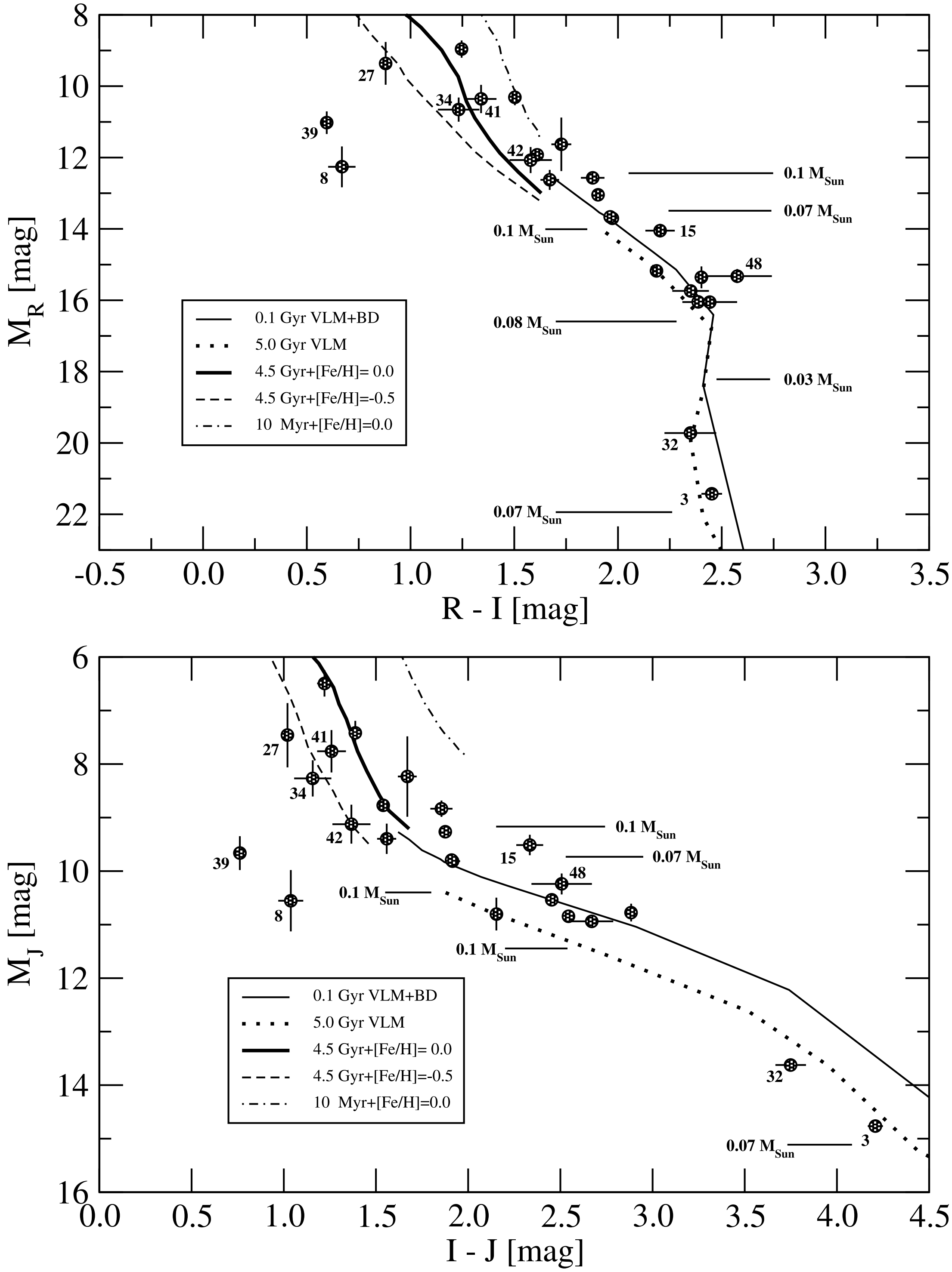

FIG. 2.—Selected CMDs. The top panel is based on *RI* data obtained in the present survey. The bottom panel combines *I*-band data from our survey with *J*-band data from 2MASS. We have superposed two sets of solar-metallicity ($Z = 0.019$, $[\mathrm{Fe/H}] = 0$) isochrones for VLMs and BDs from models by Chabrier et al. (2000). The thin solid line is for 0.1 Gyr objects (VLM+BD), and the dotted line is for 5.0 Gyr objects (VLM). For illustration purposes we have included a few mass values from the models in the figures (mass labels to the right correspond to the 0.1 Gyr isochrones; those to the left correspond to the 5.0 Gyr isochrones). We also present isochrones for 4.5 Gyr solar-metallicity (*thick solid lines*), 10 Myr solar-metallicity (*dot-dashed lines*), and 4.5 Gyr Population II abundance (*dashed lines*) RDs, all from models by Baraffe et al. (1998). See text for details. The numbers on some points correspond to those given in Table 1. Stars labeled are discussed in the text.

to avoid misleading comparisons with the VLM/BD isochrones, in Figure 3 we have plotted them just to a lower mass limit of 0.1 $M_\odot$. The reason for this was that, although both sets of isochrones are from the same group of authors, they are not strictly comparable due to differences in the physics of the models. The models by Chabrier et al. (2000) are supposed to supersede those by Baraffe et al. (1998). To illustrate the effects of age and metallicity on the Baraffe et al. (1998) RD isochrones we have also superposed a 10 Myr solar-metallicity RD isochrone (*dot-dashed line*) and a 4.5 Gyr Population II abundance RD isochrone (*dashed line*). Numbers for individual stars in Figure 2 (and also in Figs. 3 and 4; see below) are those from Table 1.

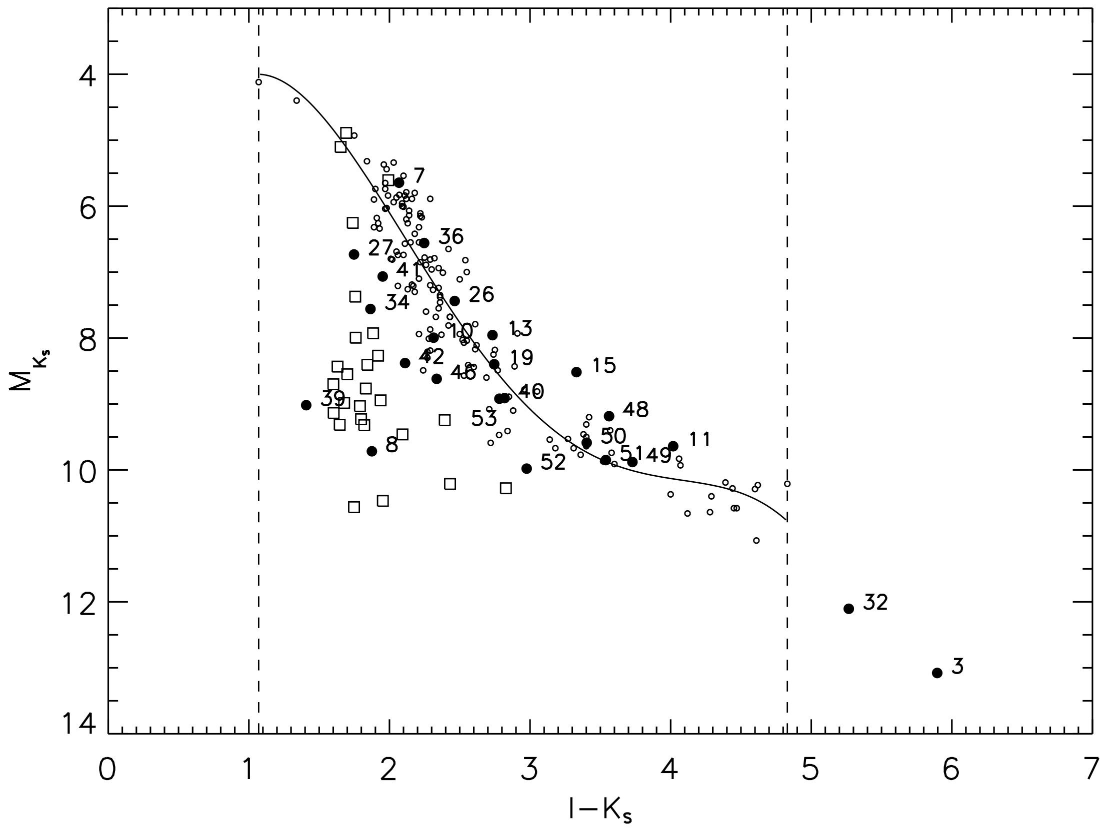

FIG. 3.—M_{K_S} vs. $I - K_S$ CMD, constructed by combining data from various sources, which illustrates the position of our targets with available trigonometric parallax (*labeled, filled circles*) in relation to the RECONS sample of nearby stars (*open circles*; H04), and to the Gizis (1997) sample of SDs with $\mu \geq 1\rlap{.}''0$ yr^{-1} (*open squares*). The solid line is an empirical fit tracing the main sequence, and the dashed vertical lines indicate the valid limits of this fit. The numbers beside the filled circles are those given in Table 1.

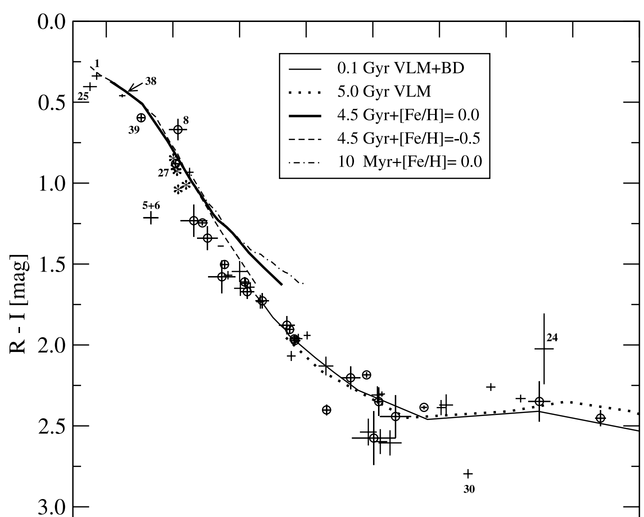

FIG. 4.—CoCoD constructed combining *RI* data obtained in the present survey with *J*-band data from 2MASS. For completeness we have superposed isochrones with the same properties as those plotted in the CMDs. It should be noted that, in contrast to Fig. 3, we have plotted all stars included in Table 1. Objects with available trigonometric parallax are depicted by circles; those without, by dots (i.e., by their error bars). The error bars represent the square root of the corresponding magnitude errors added in quadrature. The numbers given on some points correspond to those given in Table 1. Stars labeled are discussed in the text.

With the exceptions of DENIS 0255−4700 (No. 32) and 2MASS 1507−1627 (No. 3), the position of the fainter subset of our sample in the CMDs is more consistent with the 0.1 Gyr VLM+BD isochrone. Although this might *seem* to imply that we have a large sample of BDs, it should be kept in mind that such a straightforward interpretation must be taken with caution because it is difficult from CMDs alone to distinguish young BDs from solar-age VLMs. If the isochrones shown for 5.0 Gyr VLMs are systematically too faint, then most of our targets would be normal stars, as we suspect. It is of course also possible that the photometry may be affected by unknown systematic effects.

Save for two objects, IC 4756-Ref6 (No. 39) and LHS 1749-Ref4 (No.8), which are discussed below, our CMDs show no unusual features. Abundance and/or age variations can explain well the overall dispersion around the RD 4.5 Gyr solar-metallicity isochrone. Of the four stars that lie below the RD main sequence in the M_J versus $I - J$ CMD, LHS 360 (No.27), LHS 3141AB (No. 34), LHS 3451A (No. 41), and LHS 3451B (No. 42), only LHS 360 is clearly located in the SD domain in the M_R versus $R - I$ CMD and has indeed been positively identified as a M0.0 VI SD by L06 (see Table 1). LHS 3141AB is blended at the scale of the available photometry, so its position in the CMDs and in the CoCoD must be interpreted with caution.

A look at Table 7, which gives tangential velocities ($v_{\rm tan}$) for all targets with trigonometric parallaxes—along with other derived properties, including their distances and their M_R and M_J absolute magnitudes—shows that LHS 360 has a very high $v_{\rm tan}$, also indicative of its Population II nature. Accounting for errors in the parallax and the proper motion, the 1 σ range for its tangential velocity turns out to be $v_{\rm tan} = 524.4^{+202.5}_{-115.0}$ km s^{-1}. This

TABLE 7
DERIVED PROPERTIES OF OBJECTS WITH FINAL TRIGONOMETRIC PARALLAXES

Name	Distance (pc)	v_{tan} (km s^{-1})	M_R (mag)	M_J (mag)
DENIS 0255−4700	5.0	27.0	21.4	14.8
LHS 1749 AB	22.0	87.3	9.0	6.5
LHS 1749-Ref4	50.0	4.8	12.3	10.6
WT 207	24.7	74.1	11.9	8.8
LHS 2021	16.7	53.3	16.0	10.8
LP 844-33	23.6	46.4	12.6	8.8
2MASS 0952−1924	29.5	16.6	14.0	9.5
LHS 2400	22.6	65.8	13.0	9.3
LP 796-012	62.7	130.2	11.6	8.2
LHS 360	96.8	524.4	9.4	7.5
2MASS 1507−1627	6.9	29.7	19.7	13.6
LHS 3141AB	32.6	85.9	10.7	8.3
LTT 6962	38.8	112.7	10.3	7.4
IC 4756-Ref6	51.3	2.1	11.0	9.7
CE 507	15.3	28.5	13.7	9.8
LHS 3451A	44.9	107.9	10.4	7.8
LHS 3451B	41.2	102.4	12.1	9.1
LHS 505	27.9	138.1	12.6	9.4
2MASS 2206−2047	26.7	4.5	15.3	10.2
2MASS 2306−0502	12.1	59.5	16.1	10.9
APMPM J2330−4737	13.8	73.4	15.2	10.5
APMPM J2331−2750	14.5	52.4	15.7	10.8
APMPM J2344−2906	30.9	59.8	15.4	10.8
APMPM J2359−6246	20.8	57.2	13.7	9.8

value is actually quite close to the escape velocity from the solar neighborhood of approximately 620 km s^{-1} (Binney & Merrifield 1998). A tentative radial velocity consistent with an absolute value smaller than 30 km s^{-1} was determined from low-resolution spectroscopy (L06) by means of the three Ca triplet lines at 8500 Å.

In Figure 3 we present an M_{K_S} versus $I - K_S$ CMD, constructed by combining data from various sources, which illustrates the position of our targets with available trigonometric parallax (*filled circles*) in relation to the RECONS sample of nearby stars (*open circles*; Henry et al. 2004) and to the Gizis (1997) sample of SDs with $\mu \geq 1''.0$ yr^{-1} (*open squares*). The solid line is an empirical fit tracing the main sequence, and the dashed vertical lines indicate the valid limits of this fit. Examination of this figure shows that the four objects discussed in the above paragraphs are located in or close to the SD domain (as defined by the Gizis sample). We lack spectra for LHS 3451A and LHS 3451B, but they can be considered as SD candidates. The positions of IC 4756-Ref6 and LHS 1749-Ref4 in this diagram again suggest extreme properties. Two stars are seen to lie clearly above the main sequence: 2MASS 0952−1924 (No. 15) and, to a lesser extent, 2MASS 2206−2047 (No. 48). A comparison of their true (trigonometric) distances (29.5 and 26.7 pc, respectively; see Table 7) with their photometric distances calculated using the H04 relationships (18.1 pc and 18.9 pc, respectively; not included in Table 6), in the sense of D_{phot} minus D_{true}, gives a large negative percentage difference (~39% and ~29%, respectively) that, considering that both stars are confirmed main-sequence dwarfs, suggests that they may be unresolved multiples (a significant light contribution from an unknown secondary leads to an underestimation of D_{phot}). Interestingly (see Fig. 2), 2MASS 0952−1924 is clearly detached from the main sequence only in the M_J versus $I - J$ CMD. On the other hand, 2MASS 2206−2047 is clearly detached only in the M_R versus $R - I$ CMD.

In Figure 4 we present a CoCoD constructed combining our *RI* data with *J*-band data from 2MASS (other color-color combinations we tested did not show significant differences). For completeness we have superposed isochrones with the same properties as those used in the CMDs. It should be noted that, in contrast to our CMDs, in the CoCoD we have plotted all stars included in Table 1. Objects with available trigonometric parallax are depicted by circles; those without, by dots (i.e., by their error bars). The error bars represent the square root of the corresponding magnitude errors added in quadrature.

It should be noted that IC 4756-Ref6 (No. 39) and LHS 1749-Ref4 (No. 8) are clearly located in the region of the CoCoD occupied by known SDs in the complete 1.5 m CTIOPI sample: LHS 360 (No. 27; this work), and LHS 148, LHS 162, WT 233, LHS 367, and APMPM J2204−3348 (from C05; Fig. 4, *asterisks*). The other three objects in the uppermost left part of Figure 4 are LHS 339 (No. 25), a known WD; GJ 2014 (No. 1), a suspected SD (J. P. Subasavage et al. 2006, private communication); and IC 4756-H165 (No. 38), which, based on its position in the CMDs presented by Herzog et al. (1975), seems to be an early-type main-sequence star.

The facts presented here, in combination with the data presented by Reid & Gizis (2005) for extreme subdwarfs (eSDs), leads us to believe that IC 4756-Ref6 and LHS 1749-Ref4 could be eSDs. If this is indeed the case, they would be among the most extreme cases of SDs known. Because these two objects were identified serendipitously, they were not targeted by the spectroscopic survey of L06, but we expect to obtain spectra for them in the near future. Please note that, on account of their very small v_{tan}, they escaped a proper-motion-limited selection in the field of IC 4756 and LHS 1749.

We would finally like to draw attention to the few objects (most notably DENIS 1441−0945 [No. 30], for which we lack a trigonometric parallax) that are greatly detached from the color-color locus. Careful examination of the photometric data available for them suggests that in some cases the declared photometric errors alone cannot account for their position in the CoCoD. This leads us to believe that variability effects are partially responsible for the scatter. It should be noted that LHS 189/190 (Nos 5 and 6) and DENIS 1228−1547 (No. 24) are double systems, blended at the scale of the available photometry, so their position in the CoCoD cannot be interpreted directly.

7. CONCLUSIONS

We summarize here the main conclusions of this work.

1. We present 25 trigonometric parallaxes from the 1.5 m CTIOPI program. Twenty-four are of nearby star candidates, and one is of a zero-parallax calibration field. We provide the first parallaxes for 23 stellar systems.
2. Of the 23 systems with first trigonometric parallaxes reported here, one (DENIS 0255−4700) is within 10 pc, the horizon of the Research Consortium on Nearby Stars, and 10 systems are between 10 and 25 pc, the classical distance limit of the Catalog of Nearby Stars and the NStars Project.
3. At a distance of 4.97 ± 0.10 pc, and with a spectral type of L7.5 V, DENIS 0255−4700 is now the closest known L dwarf. In addition, with $M_V = 24.44$, it is the faintest dwarf with a measured absolute visual magnitude. DENIS 0255−4700 is a promising object for upcoming extrasolar planetary searches from space.
4. We present, in addition, preliminary trigonometric parallaxes for five systems, most of which clearly deserve follow-up. For four of these objects we also obtained $VRIJHK_S$-based photometric distance estimates.
5. We present $VRIJHK_S$-based photometric parallaxes for 21 objects in the 1.5 m CTIOPI input list for which it was not

possible to carry out trigonometric parallax observations. Thirteen seem to lie at distances less than 25 pc and therefore are of interest to nearby star studies.

6. Our color-magnitude and color-color diagrams, in combination with theoretical isochrones, have aided in identifying the nature of most of our targets. We have in this way discovered one new (spectroscopically confirmed) SD and two suspected eSDs that could be among the most extreme cases of these objects. We have also discovered several very low mass stars, a few of which could be BDs.

7. Our results directly contribute to improving the colors and luminosities of the lower main-sequence stars and to the quest of completing the nearby star census. By expanding the database for the solar neighborhood stars, they also contribute to investigations of the luminosity function, mass function, and kinematics of the stars in the vicinity of our Sun.

E. C. and R. A. M. acknowledge support by the Fondo Nacional de Investigación Científica y Tecnológica (project 1010137, FONDECYT) and by the Chilean Centro de Astrofísica FONDAP (15010003). This project has made generous use of the 10% Chilean time. The early phase of CTIOPI was supported by the NASA/NSF Nearby Stars Project through NASA Ames Research Center. The RECONS team at Georgia State University (GSU) is supported by NASA's Space Interferometry Mission, the NSF, and GSU. We thank Gaspare Lo Curto for his assistance in determining the spectral types given here in advance of publication. This work has used data products from the Two Micron All Sky Survey, which is a joint project of the University of Massachusetts and the Infrared Processing and Analysis Center at the California Institute of Technology funded by NASA and the NSF, and data products from DENIS, which is the result of a joint effort involving several institutes mostly located in Europe. They are supported mainly by the French Institut National des Sciences de l'Univers, CNRS, the French Education Ministry, the European Southern Observatory, the State of Baden-Wuerttemberg, the European Commission under networks of the SCIENCE and Human Capital and Mobility programs, the Landessternwarte, Heidelberg, l'Institut d'Astrophysique de Paris, the Institut fur Astrophysik der Universitat Innsbruck, and the Instituto de Astrofisica de Canarias.

REFERENCES

Arias, E. F., Charlot, P., Feissel, M., & Lestrade, J.-F. 1995, A&A, 303, 604
Baraffe, I., Chabrier, G., Allard, F., & Hauschildt, P. H. 1998, A&A, 337, 403
Bergeron, P., Leggett, S. K., & Ruiz, M. T. 2001, ApJS, 133, 413
Bertin, E., & Arnouts, S. 1996, A&AS, 117, 393
Binney, J., & Merrifield, M. 1998, Galactic Astronomy (Princeton: Princeton Univ. Press)
Bucciarelli, B., et al. 2001, A&A, 368, 335
Chabrier, G., Baraffe, I., Allard, F., & Hauschildt, P. 2000, ApJ, 542, 464
Costa, E., & Méndez, R. A. 2003, A&A, 402, 541
Costa, E., Méndez, R. A., Jao, W.-C., Henry, T. J., Subasavage, J. P., Brown, M. A., Ianna, P. A., & Bartlett, J. 2005, AJ, 130, 337 (CO5)
Dahn, C. C., et al. 2002, AJ, 124, 1170 (DO2)
Gizis, J. E. 1997, AJ, 113, 806
Graham, J. A. 1982, PASP, 94, 244
Henry, T. J., Subasavage, J. P., Brown, M. A., Beaulieu, T. D., Jao, W., & Hambly, N. C. 2004, AJ, 128, 2460 (HO4)
Henry, T. J., Walkowicz, L. M., Barto, T. C., & Golimowski, D. A. 2002, AJ, 123, 2002
Herzog, A. D., Sanders, W. L., & Seggewiss, W. 1975, A&AS, 19, 211
Jao, W., Henry, T. J., Subasavage, J. P., Bean, J. L., Costa, E., Ianna, P. A., & Méndez, R. A. 2003, AJ, 125, 332
Jao, W.-C., Henry, T. J., Subasavage, J. P., Brown, M. A., Ianna, P. A., Bartlett, J. L., Costa, E., & Méndez, R. A. 2005, AJ, 129, 1954
Jefferys, W. H., Fitzpatrick, M. J., & McArthur, B. E. 1987, Celest. Mech., 41, 39
Landolt, A. U. 1992, AJ, 104, 340
Lodieu, N., Scholz, R.-D., McCaughrean, M. J., Ibata, R., Irwin, M., & Zinnecker, H. 2005, A&A, 440, 1061
Martin, E. L., Brandner, W., & Basri, G. 1999, Science, 283, 1718
Reid, I. N., & Gizis, J. E. 2005, PASP, 117, 676
Salim, S., Rich, R. M., Hansen, B. M., Koopmans, L. V. E., Oppenheimer, B. R., & Blandford, R. D. 2004, ApJ, 601, 1075
Scholz, R.-D., Ibata, R., Irwin, M., Lehmann, I., Salvato, M., & Schweitzer, A. 2002, MNRAS, 329, 109
Wroblewski, H., & Costa, E. 2001, A&A, 367, 725